Schreuder, H. A., van der Laan, J. M., Thunniseen, M. M. G. M., Kak, K. H., Swarte, M. B. A., Hol, W. G. J., & Drenth, J. (1987) in *Flavins and Flavoproteins* (Edmondson, D. E., & McCormick, D. B., Eds.) pp 527–538, Walter de Gruyter, Berlin.

Spencer, R., Fisher, J., & Walsh, C. (1976) *Biochemistry 15*, 1043–1053.

Stewart, R. C., & Massey, V. (1985) *J. Biol. Chem. 260*, 13639–13647.

Sullivan, P. A., Choong, Y. S., Schreurs, W. J., Cutfield, J. F., & Shepherd, M. G. (1977) *Biochem. J. 165*, 375–383.

Swoboda, B. E. P., & Massey, V. (1965) *J. Biol. Chem. 240*, 2209–2215.

Van den Berghe-Snorek, S., & Stankovich, M. (1985) *J. Biol. Chem. 260*, 3373–3379.

Van Schagen, C. G., & Müller, F. (1981) *Eur. J. Biochem. 120*, 33–39.

Vervoort, J. (1986) Ph.D. Dissertation, Agricultural University, Wageningen, The Netherlands.

Vervoort, J., Müller, F., Mayhew, S. G., van den Berg, W. A. M., Moonen, C. T. W., & Bacher, A. (1986) *Biochemistry 25*, 6789–6799.

Weber, G. (1950) *Biochem. J. 47*, 114–121.

Wierenga, R. K., de Jong, R. J., Kalk, K. H., Hol, W. G. J., & Drenth, J. (1979) *J. Mol. Biol. 131*, 55–73.

Structure of Interleukin 1α at 2.7-Å Resolution†

Bradford J. Graves,*,‡ Marcos H. Hatada,‡ Wayne A. Hendrickson,§ Julann K. Miller,‡ Vincent S. Madison,‡ and Yoshinori Satow‖

Roche Research Center, Hoffmann-La Roche Inc., Nutley, New Jersey 07110, Howard Hughes Medical Institute, Department of Biochemistry and Molecular Biophysics, Columbia University, New York, New York 10032, and Faculty of Pharmaceutical Sciences, University of Tokyo, Hongo, Bunkyo-ku, Tokyo 113, Japan

Received September 8, 1989; Revised Manuscript Received October 9, 1989

ABSTRACT: The interleukin 1 (IL-1) family of proteins has a central role in modulating immune and inflammatory responses. Two major IL-1 proteins, designated α (IL-1α) and β (IL-1β), are produced by activated macrophages and other cell types. In an effort to understand the similarities and differences in the physicochemical and functional properties of these two proteins, a program was initiated to determine their structures. Crystals of IL-1α were grown, and the three-dimensional structure at 2.7-Å resolution was solved. The technique of multiple-wavelength anomalous dispersion (MAD) with the selenomethionine form of IL-1α was utilized in combination with a single mercury derivative to provide the starting phases. Partial refinement of the IL-1α model has been performed as well. The overall structure is composed of 14 β-strands and a 3_{10} helix. The core of this structure is a capped β-barrell that possesses 3-fold symmetry and displays a topology similar to that observed for IL-1β [Priestle, J. P., et al. (1988) *EMBO J. 7*, 339–343] and soybean trypsin inhibitor (STI) [McLachlan, A. D. (1979) *J. Mol. Biol. 133*, 557–563]. In this paper, the overall structure of IL-1α and the nature and fidelity of the internal 3-fold symmetry are discussed. Comparisons with IL-1β and STI are made within these contexts.

Interleukin 1 (IL-1) molecules found in serum are relatively small proteins of approximately 17 500 daltons and are thought to be involved in the initiation or exacerbation of a number of disease states including rheumatoid arthritis (Dinarello, 1984; Oppenheim et al., 1986; Lomedico et al., 1986). The cDNAs encoding human IL-1α and IL-1β have been sequenced (Auron et al., 1984; March et al., 1985; Gubler et al., 1986), showing that both proteins are synthesized as larger precursor molecules. The primary structures of the IL-1α and IL-1β precursors have several common features: (1) they are approximately the same size (271 and 269 amino acids, respectively), (2) they lack a classical signal peptide sequence, and (3) the IL-1 bioactivity maps to the carboxy-terminal half of the precursor. Among various mammalian species, IL-1α proteins are all between 60% and 70% identical in sequence to one another. Similar sequence identity has been noted for the IL-1β proteins. However, there is less than 30% sequence identity between IL-1α and IL-1β proteins. Despite marked differences in amino acid sequences, both IL-1α and IL-1β appear to have similar, if not identical, biological activities (Rupp et al., 1986) as they bind to the same receptor protein (Dower et al., 1986a,b; Kilian et al., 1986; Matsushima et al., 1986) with similar affinities on target cells. IL-1α and IL-1β do differ in certain physicochemical properties [e.g., isoelectric points (Schmidt, 1984; Saklatvala et al., 1985) and sensitivity to heat (Krakauer, 1985)], but they exhibit similar NMR and CD spectra (Gronenborn et al., 1986; Craig et al., 1987; D. C. Fry, personal communication).

We have undertaken the solution of the three-dimensional structure of a recombinant form of human IL-1α as part of a drug discovery program. We have also used this project in an effort to demonstrate the feasibility of utilizing selenomethionine forms of proteins with the multiple-wavelength anomalous dispersion (MAD) method for solving protein structures without heavy-atom derivatives (Hendrickson, 1985). We report herein the crystal structure of IL-1α at 2.7-Å resolution.

Experimental Procedures

The purification of IL-1α followed standard chromatographic techniques as detailed elsewhere (Roy et al., 1989).

† The Cα coordinates have been deposited in the Brookhaven Protein Data Bank (code 1ILA).

* To whom correspondence should be addressed.
‡ Roche Research Center.
§ Columbia University.
‖ University of Tokyo.

0006-2960/90/0429-2679$02.50/0

Table I: Heavy-Atom Refinement Parameters

	resolution (Å)								
	14.1	9.2	6.8	5.4	4.5	3.8	3.4	3.0	total
native									
no. of observations	30	75	153	243	370	523	680	858	2932
figure of merit	0.76	0.82	0.87	0.80	0.80	0.80	0.75	0.67	0.75
CMB									
rms F_H/residual[a]	3.05	3.44	3.03	3.44	3.63	2.52	2.43	2.50	3.00
R cullis[b]	0.37	0.25	0.32	0.35	0.33	0.61	0.58	0.84	0.45

	mercury position				
	X	Y	Z	occupancy (e)	B (Å^2)
Hg	0.442	0.000	0.237	57.7	22.8

[a] rms F_H/residual = $\{\sum F_H^2/\sum[F_{pH}(\text{obs}) - F_{pH}(\text{calcd})]^2\}^{1/2}$. [b] R cullis = $\sum|F_{pH}(\text{obs}) - F_{pH}(\text{calc})|/\sum|F_{pH}(\text{obs}) - F_p(\text{obs})|$ for centric reflections, where F_p, F_H, and F_{pH} = structure factor amplitude for parent, heavy atom, and derivative, respectively.

The selenomethionine form of IL-1α (Se-Met IL-1α) was produced via established procedures (Cowie & Cohen, 1957; Hendrickson et al., unpublished results) and purified under the same conditions as for normal IL-1α. Crystals of IL-1α were grown by the vapor diffusion method using a 1:1 mixture of reservoir and protein solutions. The protein concentration was 35 mg/mL, and the reservoir contained 0.1 M citrate, 0.2 M ammonium acetate, and 30% (w/v) poly(ethylene glycol) 4000, pH 6.2. In order to increase reproducibility, the protein drops were seeded with small crystals. The only usable heavy-atom derivative was obtained with the thiol titrating reagent *p*-(chloromercuri)benzoate (*p*-CMB). A modification of the technique outlined by Boyer (1954) was employed: Dilute (~1 mg/mL) protein was dialyzed for 72 h against 100 mL of 100 μM *p*-CMB, followed by extensive dialysis against buffer to remove excess heavy-metal reagent. The absorbance spectrum between 240 and 290 nm of the treated protein (normalized to that of native protein on the basis of the A_{290}) was used to assess the level of mercury binding. Crystals were grown from the derivatized protein. Soaking preformed IL-1α crystals with a wide variety of mercurial compounds always resulted in either cracked crystals or no derivatization.

Diffraction data on native and mercury derivative IL-1α crystals were collected at room temperature on an Enraf Nonius CAD4 diffractometer. Monochromatized Cu Kα radiation was used, and data, including Friedel pairs for the mercury derivative, were measured with a continuous ω-scan. Only one crystal in each case was required for complete data sets (to 2.7- and 3.0-Å resolution for native and derivative data, respectively) with crystal decay of less than 15%. Correction for crystal decay was based on periodic measurements of several standard reflections, and a semiempirical absorption correction (North et al., 1968) was made by using ψ-scans of reflections with χ values near 90°.

Data from the crystals of Se-Met IL-1α were collected on the diffractometer facility on beam-line 14A at the Photon Factory. The experimental design was patterned on that used in an earlier MAD experiment with selenobiotinylstreptavidin (Hendrickson et al., 1989). Data were measured from three crystals (approximate size 0.4 × 0.25 × 0.05 mm) of Se-Met IL-1α in shells starting from low scattering angles with a succession of four wavelengths (three for the last crystal) within each shell. The choice of wavelengths relative to the selenium absorption edge, which was measured by X-ray fluorescence spectroscopy, was made in analogy with a MAD phasing test on lamprey hemoglobin (Hendrickson et al., 1988). The diffraction data were reduced with corrections for background, attenuator absorption, beam monitor normalization, ψ-scan absorption, and Lorentz and polarization factors (program by Y. Satow). A unique set of data collected on Se-Met IL-1α crystals with Cu Kα radiation and scaled by Wilson's statistics was used to place the Photon Factory data on an absolute scale and to correct for radiation damage. Algebraic analysis (Karle, 1980) by the program MADLSQ (Hendrickson, 1985; Hendrickson et al., 1988, 1989) led to a set of $|^{\circ}F_A|$, $|^{\circ}F_T|$, and $(^{\circ}\phi_T - {}^{\circ}\phi_A)$ data for all 2406 reflections in the range of Bragg spacings between 12.5 and 3.3 Å. Calculated selenium phases, $^{\circ}\phi_A$, together with MADLSQ results were then used to derive *ABCD* coefficients to permit phase combination with mercury SIR results. Unit weights were applied to the SIR and MAD phases for combination. Finally, these combined phases were extended from 3.0 to 2.7 Å with a program by Wang (1985).

Results and Discussion

The crystals of recombinant, human IL-1α belong to the space group $P2_1$ in the monoclinic system with cell constants a = 31.97 Å, b = 54.52 Å, c = 45.63 Å, and β = 108.63°, and they diffract to better than 2-Å resolution. Assuming one molecule in the asymmetric unit with a molecular mass of 17 689 daltons, a Matthews coefficient (Matthews, 1968) of 2.13 was calculated which corresponds to a solvent content of 42%. As judged by unit cell dimensions (a = 32.06 Å, b = 54.50 Å, c = 45.81 Å, and β = 108.63°), the crystals of Se-Met IL-1α appear to be essentially isomorphous with those of the natural protein. On the other hand, the Se-Met IL-1α protein is less soluble, and the crystals have a higher tendency toward physical twinning. The crystals used for the MAD data collection were affected by this characteristic. The crystals of *p*-CMB IL-1α have unit cell constants nearly identical with those of the native protein, and diffractometer scans of axial reflections clearly indicate major shifts in relative intensities. On the basis of the extinction coefficients of a *p*-CMB–S complex (Boyer, 1954) and IL-1α, it appears that the protein is 100% derivatized.

The quality of the diffraction data for the native and mercury derivative crystals appears to be quite high. The native and derivative data sets have R_{sym} (on I) values of 0.026 and 0.033, respectively. The merging R-factor between the data sets is 0.18 to 3.0-Å resolution. The mercury position was determined from isomorphous and anomalous difference Patterson maps with the mercury peak being the largest peak (at 19σ and 11σ, respectively) in the Harker section. The heavy-atom refinement statistics are shown in Table I.

The multiple-wavelength data also possess reasonable internal agreement with R_{sym} (on I) values at the individual wavelengths of 0.03–0.04. But the reflection profiles were broad and highly structured. The pattern of average Bijvoet and dispersive differences is roughly consistent with the theoretical expectation (see Table II), but the error level is appreciably higher than was observed with selenobiotinylstreptavidin (Hendrickson et al., 1989). These errors may be

Table II: Anomalous Diffraction Signals from the Photon Factory MAD Experiment[a]

	obsd ratios (d = 12.5–3.9 Å)				obsd ratios (d = 3.9–3.3 Å)			expected ratios (d = ∞)				scattering factors	
λ (Å)	0.9000 Å	0.9784 Å	0.9795 Å	1.1000 Å	0.9000 Å	0.9784 Å	0.9795 Å	0.9000 Å	0.9784 Å	0.9795 Å	1.1000 Å	f'	f''
0.9000	0.076 (0.064)	0.062	0.074	0.078	0.071 (0.090)	0.061	0.065	0.030	0.029	0.035	0.002	−1.622	3.284
0.9784		0.074 (0.052)	0.049	0.066		0.075 (0.092)	0.048		0.032	0.006	0.027	−7.898	3.492
0.9795			0.060 (0.049)	0.073			0.061 (0.060)			0.023	0.033	−9.231	2.478
1.1000				0.058 (0.070)							0.006	−1.957	0.617

	selenium positions[b]				
	X	Y	Z	occupancy (%)	B (Å^2)
Se1	0.633	0.110	0.603	0.86	10.0
Se2	0.943	0.159	0.991	0.86	20.0
Se3	0.397	0.417	0.295	0.86	10.0

[a] Bijvoet difference ratios (Hendrickson et al., 1985) are given in diagonal elements with centric values in parentheses. Dispersive difference ratios (Hendrickson et al., 1985) are given as the off-diagnoal elements. Observed Bijvoet and dispersive difference ratios were computed as $\text{rms}(\Delta F\pm_h)/\text{rms}(|F|)$ and $\text{rms}(\Delta F_A\lambda)/\text{rms}(|F|)$, respectively. The expected values were computed as $s[2f''(\lambda)]$ for diagnoal elements and $s|f' - f'(\lambda_j)|$ for off-diagonal elements, where $s = q(N_A)^{1/2}/[(2N_T)^{1/2}Z_{eff}]$. Z_{eff} = 6.7 e is the effective normal atomic scattering at zero scattering angle, N_T = 1160 is the approximate number of non-hydrogen atoms in IL-1α, N_A = 3 is the number of assumed selenium sites, and q = 0.86 is the selenium occupancy factor. Scattering factors at the absorption edge were evaluated in a MAD fitting program (Y. Satow, unpublished), and those at remote wavelengths were computed from theoretical cross sections (Cromer, 1983). [b] Least-squares refinement of the selenium positions using a selected set of reflections was performed as described by Hendrickson et al. (1989) for selenobiotinylstreptavidin and gave an R-factor of 0.361.

Table III: Alignment of β-Strands[a] in the Common Motif[b] for IL-1α and STI and Equivalent Atoms in Superposition for IL-1α

Version	Strand 1	Strand 2	Strand 3	Strand 4
IL-1α A	^{14}i k **Y E F I L N D A**^{23}	^{24}l n **Q S I I R** a n d^{33}	^{34}**Q Y L T A A** a^{40}	^{48}**V K F D M G A Y** k s s^{58}
IL-1α B	^{59}k d **D A K I T V I L**^{68}	^{69}r i s **K T Q L Y** v t a q^{80}	^{81}d e d **Q P V L L K** e m^{91}	^{105}**L L F F W E T H** g^{113}
IL-1α C	^{114}**T K N Y F T S V**^{121}	^{122}a h p n **L F I A T** k q^{132}	^{133}d **Y W V C L A** g^{140}	^{146}**T D F Q I L E N**^{153}
STI A	^{14}g **G T Y Y Y I L S D** i t^{24}	^{25}a g **F G I R A** a p t g^{35}	^{36}n e r c p **L T V V Q S** r n^{48}	^{51}d k g **I G T I I S P S** y^{62}
STI B	^{71}**H P L S L K R D** s f a^{81}			

matches	total equivalences	rms (Å)	rotation angle (deg)	axial translation (Å)
A–B, B–C, and C–A	81	1.54	120.2	0.00
A–B	27	1.26	123.2	−0.46
B–C	27	1.32	117.0	0.05
C–A	27	1.62	120.5	0.38

[a] The alignments were based on crystallographic coordinates for IL-1α and STI (Sweet et al., 1974) strands A1–B1. For IL-1α and STI strands A1–B1, the full-length β-strands are given including the terminal hairpin turn residues. Residue numbers are given for the terminal residues in each β-strand. [b] Sequence in bold upper case.

due to the physical nature of the crystals as mentioned previously. Three of the four potential selenium positions were determined from a $|^{\circ}F_A|^2$ Patterson synthesis. These positions were refined and subsequently confirmed with protein phases obtained from the mercury derivative. Selenium coordinates relative to the mercury site are given in the legend of Table II.

It was not possible to interpret the electron density maps computed from MAD phasing of the Photon Factory data. On the other hand, the mercury SIR map was very good (figure of merit was 0.74 or 0.88 from centric or general reflection error estimates, respectively), and most of the backbone could be traced, although there were some ambiguities near the metal binding site. A figure of merit of 0.92 was calculated for the combination of the MAD and mercury SIR phases. The combined phases were extended to 2.7 Å (Wang, 1985) with an average figure of merit of 0.88 and an R-value for map inversion of 0.14. The resulting 2.7-Å minimap is free of ambiguities and enabled us to trace the entire backbone. A portion of the minimap is displayed in Figure 1. Interpretation of the map was facilitated by the identification of three of the four methionine residues (the fourth one at the amino terminus appears to be disordered). α-Carbon (Cα) positions obtained from the minimap served as a guide to create a full set of coordinates with the graphics program FRODO (Jones, 1978). The initial model included residues 6–153, with broken density at the turns between residues 32–34 and 58–60. Refinement was initiated with the program XPLOR (Brünger, 1987) using data between 5- and 2.7-Å resolution. Currently, the R-factor is 0.25 for a model that has no ordered solvent, a single, overall temperature factor, and rms deviations of 0.018 Å from bond ideality and 6.0° for the ω torsion angle. Our current model of IL-1α includes all residues from sequence positions 3–153. Further refinement and rebuilding of the model are in progress.

The secondary structure of IL-1α consists almost entirely of antiparallel β-sheet. The core of this structure is a six-stranded β-barrel that is closed at one end by another six β-strands to form a bowl-like structure. Figure 2 is a view of this structure down the barrel axis. There are additional secondary structural elements in IL-1α that elaborate the basic

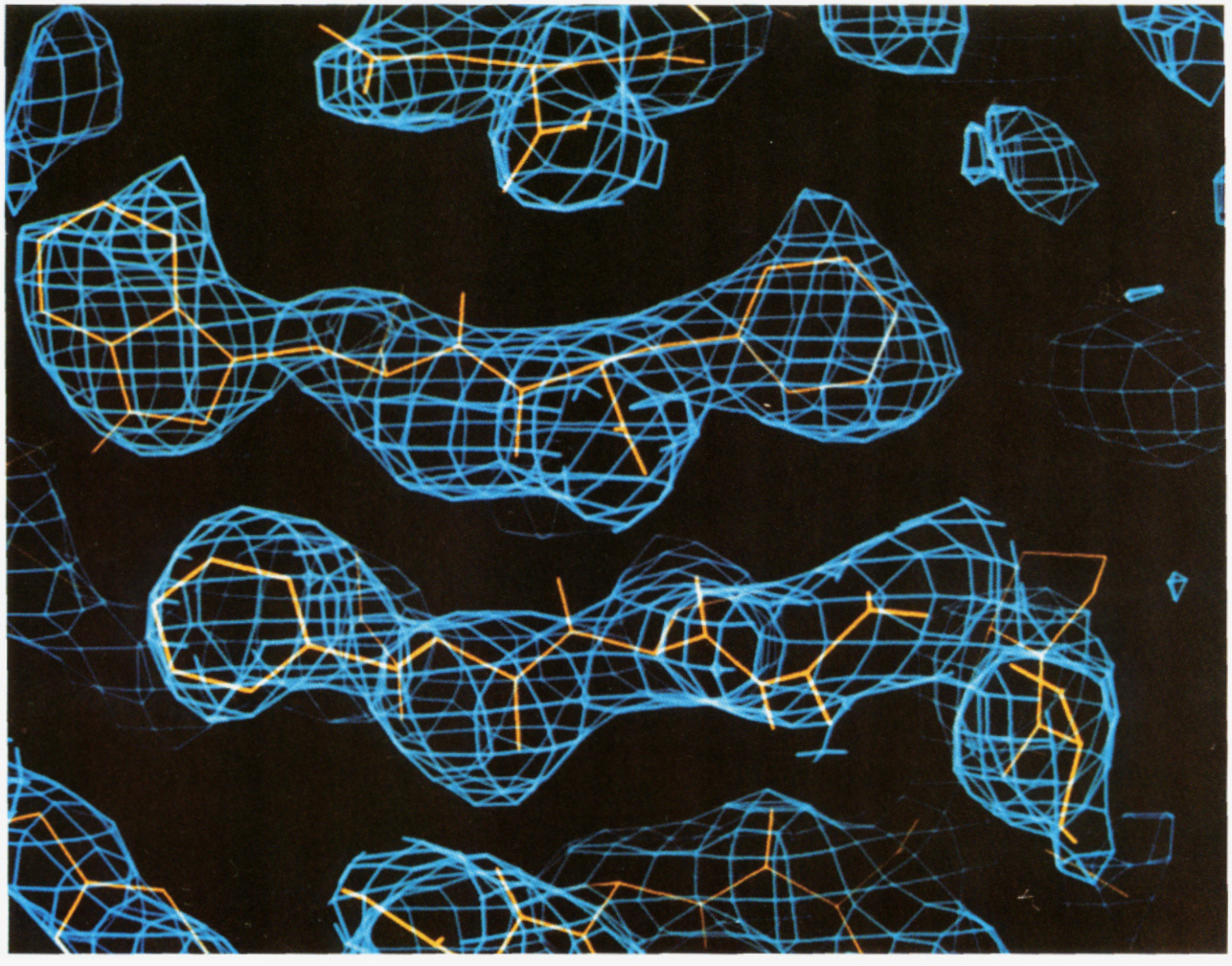

FIGURE 1: View of a section of the electron density map used for fitting the structure of IL-1α with the associated parts of the model: Phe^{108} and Trp^{109} on the top strand and Phe^{118}–Ser^{120} on the bottom strand. Phases were derived from phase combination of the selenium MAD and mercury SIR phases and extended to 2.7-Å resolution. The map is contoured at 0.35 e/Å^3. The model includes amide hydrogens as a result of refinement with XPLOR.

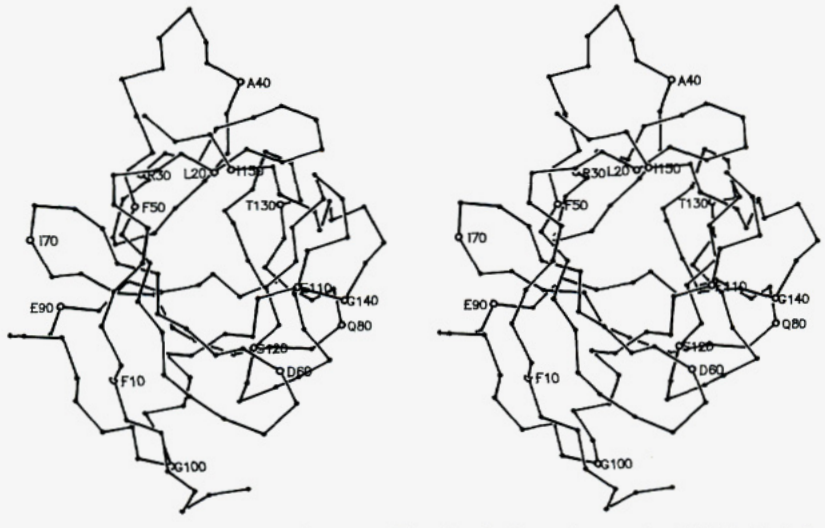

FIGURE 2: Stereoview of the Cα-backbone representation of IL-1α. The view is down the pseudo 3-fold axis defined by the superposition of 81 residues. Every tenth residue is labeled. The protein used in this investigation was synthesized in *Escherichia coli* and was derived from a clone that coded for residues 118–271 of the precursor protein and included an N-terminal methionine. The residues are thus numbered 1–155, and the sequence begins with Met^1-Phe^2-Leu^3-Ser^4.

β-barrel core: a short β-strand near the N-terminus (residues 6–10), which will be called strand N, another short β-strand (strand BL, residues 97–99), and about two turns of 3_{10} helix (residues 101–105). Complete residue assignments for all β-strands are given in Table III.

A striking feature of the structural core is that it has nearly exact internal 3-fold symmetry. Similar 3-fold symmetry has been described qualitatively for IL-1β (Priestle et al., 1988)

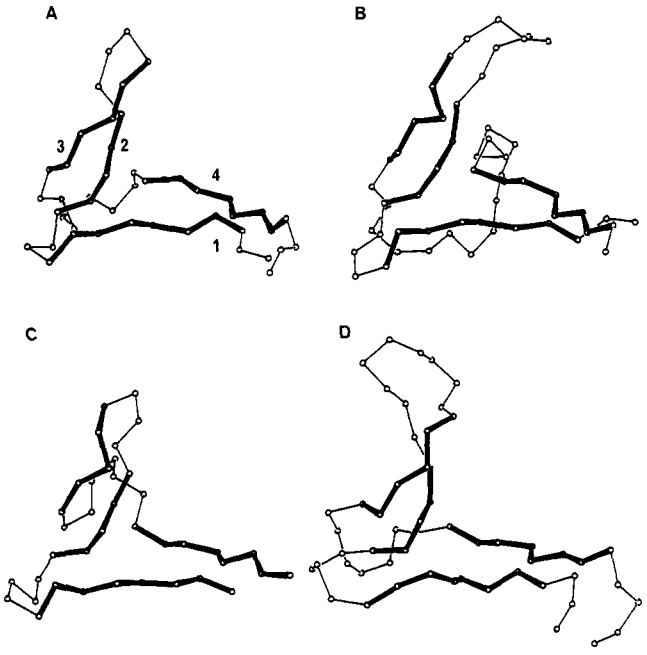

FIGURE 3: Fragments of IL-1α and soybean trypsin inhibitor (STI) showing the common structural motif composed of four β-strands. Cα positions which comprise the 27-atom common core in each version of the motif are connected by heavy lines. The identity of these residues is indicated in Table III. The four versions of the motif were overlapped by using symmetry operations indicated in the text. (A) Version A of the motif in IL-1α. Strands 1–4 are labeled. (B) Version B of the motif. (C) Version C of the motif. (D) Residues 12–65 of STI that form the same motif.

and more quantitatively for STI by McLachlan (1979). We designate the overall structure as the IL-1 fold and each unit of repeated structure as the IL-1 motif. Proceeding in order from the N- to the C-terminus of IL-1α, the three versions of the IL-1 motif are labeled A, B, and C. Each repeat unit has four β-strands, numbered 1–4 in order (A1, A2, A3, A4; B1, B2, ...). Strands A1, A4, B1, B4, C1, and C4 have extended antiparallel regions in contact to form the β-barrel. These strands form hydrogen bonds with their neighbors in the above list in an up–down topology (Richardson, 1981) completed by C4–A1 interactions. The remaining six strands in the core structure (A2, A3, B2, B3, C2, and C3) cap the end of the barrel. Assignment for topologically equivalent residues in each of these 12 strands are given in Table III.

A quantitative comparison of the geometry of the Cα atoms in the three versions of the common motif of IL-1α was performed by an iterative least-squares procedure (Hendrickson, 1979). Several starting sets were investigated to assure the validity of the equivalences at convergence. The final best-fit for the triads (Table III) shows that there are a total of 81 common atoms related by the 3-fold pseudo symmetry within a root mean square (rms) distance of 1.54 Å and that the rotation angle is 120.2° with no translational component. All of the equivalent Cα's are located within the β-strands, and 70% of the residues in the β-strands are included. Figure 3 depicts the similarity of the three versions of the motif in IL-1α. Pairwise comparisons show that each version is related to the next by a pseudo-screw rotation of about 120°, a small axial shift, and small rms deviations (1.26–1.62 Å). β-Strands of the IL-1 motifs are remarkably similar in spite of their uniquely twisted arrangement. However, there is considerable diversity among related loops. Only two symmetry-related connections in IL-1α have the same length, and even these have different conformations. In all three versions, hairpin turns connect strands 1 to 2, 2 to 3, and 4 to 1 (e.g., A1–A2, A2–A3, and A4–B1) with the differences in loop length taken up in β-strand extensions. Strands 3 and 4 are connected by longer loops that vary considerably from version to version in both length and conformation.

There is very little internal similarity to accompany the 3-fold structural similarity among the IL-1 motifs. Pairwise comparisons within IL-1α, for example, show only three identities (11%). Despite this lack of sequence similarity, the 3-fold symmetry exists with high fidelity: 1.54 Å rms for IL-1α and 2.1 Å rms for STI (McLachlan, 1979). For comparison, the 2-fold duplications within myohemerythrin, parvalbumin, bacterial ferredoxin, and lactate dehydrogenase (Hendrickson & Ward, 1977) exhibit rms separations that range from 1.4 Å with 46% sequence identity for ferredoxin to 2.7 Å with 11% identity for lactate dehydrogenase.

The common motif in IL-1α was compared to that in STI on the basis of published atomic coordinates (Sweet et al., 1974). Residues 1–93 of STI correspond to version A and part of version B of the IL-1 motif. The same 27-atom common core from version A of IL-1α was matched with the equivalent positions in STI with a rms distance of 1.73 Å. An alignment of the cyclic permutation A2–4, B1 matches even better with a rms discrepancy of 1.29 Å. Again, the β-strands are equivalent (see Figure 3), but the loop regions differ considerably for STI compared to IL-1α.

As mentioned above, the structure of IL-1α includes three additional secondary structure elements that have not been reported for IL-1β. Note especially that strand N, via hydrogen bonds to strands A4 and BL, positions the N-terminus of IL-1α at a different location than that of IL-1β [cf. Figure 2 of this work and Figure 3 of Priestle et al. (1988)]. This feature may be critical in explaining one of the few major differences between IL-1α and IL-1β: both the precursor and mature forms of IL-1α bind to IL-1 receptors and exhibit biological activity while only the mature form of IL-1β is active (Moseley et al., 1987). Thus, in the case of IL-1β it would seem that additional residues at the N-terminus of the mature protein interfere with receptor binding in a direct manner (Wingfield et al., 1987) and that this region in both proteins may be close to, if not part of, the receptor binding site. Sequence identities between IL-1α and IL-1β appear to shed little additional light on receptor binding as most of the identical residues are located in the hydrophobic core and those on the surface are widely scattered. Clearly, definitive statements on this point require knowledge of the structures of the two precursors or, preferably, of the IL-1–IL-1 receptor complexes.

The structural similarity between IL-1α and IL-1β is not surprising given their parallel biological activities and primary sequence similarity. However, the fact that the unrelated protein STI has the same structural core (the IL-1 fold) suggests that the IL-1 fold will occur in other proteins and that it will be recognized as a general tertiary structure for protein domains. Future examples may include endothelial cell growth factor (ECGF) and the DE-3 trypsin/tissue plasminogen activator inhibitors. The DE-3 inhibitors exhibit high sequence identity with STI (Joubert & Dowdle, 1987), and ECGF possesses sequence similarity with the IL-1 proteins (Jaye, 1986) that is comparable to what is observed between IL-1α and IL-1β. In addition, preliminary NMR data have identified extensive β-sheet secondary structure for ECGF (D. C. Fry, personal communication) which is consistent with it having the IL-1 fold.

ACKNOWLEDGMENTS

We thank Drs. Charles Cook, Patricia Kilian, Robert Crowl,

Dale Mueller, and Swapan Roy for their valuable assistance with various stages of this project.

REFERENCES

Auron, P. E., Webb, A. C., Rosenwasser, L. J., Mucci, S. F., Rich, A., Wolff, S. M., & Dinarello, C. A. (1984) *Proc. Natl. Acad. Sci. U.S.A. 81*, 7907–7911.

Boyer, P. D. (1954) *J. Am. Chem. Soc. 76*, 4331–4337.

Brünger, A. T., Kuriyan, J., & Karplus, M. (1987) *Science 235*, 458–460.

Cowie, D. B., & Cohen, G. N. (1957) *Biochim. Biophys. Acta 26*, 252–261.

Craig, S., Schmeissner, U., Wingfield, P., & Pain, R. H. (1987) *Biochemistry 26*, 3570–3576.

Cromer, D. T. (1983) *J. Appl. Crystallogr. 16*, 437.

Dinarello, C. A. (1984) *Rev. Infect. Dis. 6*, 51–95.

Dower, S. K., Kronheim, S., Hopp, T. P., Cantrell, M., Deeley, M., Henney, C. S., Gillis, S., & Urdal, D. L. (1986a) *Nature 324*, 266–268.

Dower, S. K., Call, S. M., Gillis, S., & Urdal, D. L. (1986b) *Proc. Natl. Acad. Sci. U.S.A. 83*, 1060–1064.

Gronenborn, A. M., Clore, G. M., Schmeissner, U., & Wingfield, P. (1986) *Eur. J. Biochem. 161*, 37–43.

Gubler, U., Chua, A. O., Stern, A. S., Hellmann, C. P., Vitek, M. P., DeChiara, T. M., Benjamin, W. R., Collier, K. J., Dukovich, M., Familletti, P. C., Fiedler-Nagy, C., Jenson, J., Kaffka, K., Kilian, P. L., Stremlo, D., Wittreich, B. H., Woehle, D., Mizel, S. B., & Lomedico, P. T. (1986) *J. Immunol. 136*, 2492–2497.

Hendrickson, W. A. (1979) *Acta Crystallogr. A35*, 158–163.

Hendrickson, W. A. (1985) *Trans. Am. Crystallogr. Assoc. 21*, 11–21.

Hendrickson, W. A., & Ward, K. B. (1977) *J. Biol. Chem. 252*, 3012–3018.

Hendrickson, W. A., Smith, J. L., & Sheriff, S. (1985) *Methods Enzymol. 115*, 41–55.

Hendrickson, W. A., Smith, J. L., Phizackerley, R. P., & Merritt, E. A. (1988) *Proteins 4*, 77–88.

Hendrickson, W. A., Pähler, A., Smith, J. L., Satow, Y., Merritt, E. A., & Phizackerley, R. P. (1989) *Proc. Natl. Acad. Sci. U.S.A. 86*, 2190–2194.

Jaye, M., Howk, R., Burgess, W., Ricca, G. A., Chiu, I.-M., Ravera, M. W., O'Brien, S. J., Modi, W. S., Maciag, T., & Drohan, W. N. (1986) *Science 233*, 541–545.

Jones, T. A. (1978) *J. Appl. Crystallogr. 11*, 268–272.

Joubert, F. J., & Dowdle, E. B. D. (1987) *Thromb. Haemostasis 57*, 356–360.

Karle, J. (1980) *Int. J. Quantum Chem. 7*, 357–367.

Kilian, P. L., Kaffka, K., Stern, A. S., Woehle, D., Benjamin, W. R., DeChiara, T. M., Gubler, U., Farrar, J. J., Mizel, S. B., & Lomedico, P. T. (1986) *J. Immunol. 136*, 4509–4514.

Krakauer, T. (1985) *J. Leukocyte Biol. 37*, 511–518.

Lomedico, P. T., Kilian, P. L., Gubler, U., Stern, A. S., & Chizzonite, R. (1986) *Cold Spring Harbor Symp. Quant. Biol. 51*, 631–639.

March, C. J., Moseley, B., Larsen, A., Cerretti, D. P., Braedt, G., Price, V., Gillis, S., Henney, C. S., Kronheim, S. R., Grabstein, K., Conlon, P. J., Hopp, T. P., & Cosman, D. (1985) *Nature 315*, 641–647.

Matsushima, K., Akahoshi, T., Yamada, Y., Furutani, Y., & Oppenheim, J. J. (1986) *J. Immunol. 136*, 4496–4502.

Matthews, B. W. (1968) *J. Mol. Biol. 33*, 491–497.

McLachlan, A. D. (1979) *J. Mol. Biol. 133*, 557–563.

Moseley, B., Urdal, D. L., Prickett, K. S., Larsen, A., Cosman, D., Conlon, P. J., Gillis, S., & Dower, S. K. (1987) *J. Biol. Chem. 262*, 2941–2944.

North, A. C. T., Phillips, D. C., & Matthews, F. S. (1968) *Acta Crystallogr. A24*, 351–359.

Oppenheim, J. J., Kovacs, E. J., Matsushima, K., & Durum, S. K. (1986) *Immunol. Today 7*, 45–56.

Priestle, J. P., Shär, H. P., & Grütter, M. G. (1988) *EMBO J. 7*, 339–343.

Richardson, J. S. (1981) *Adv. Protein Chem. 34*, 167–339.

Roy, S., Russoman, E., Monkarsh, S., Kilian, P., Smart, J., & Benjamin, W. (1989) Meeting of the International Chemical Congress of Pacific Basin Societies, Honolulu, HI, Dec 17–22, Abstract 42.

Rupp, E. A., Cameron, P. M., Ranawat, C. S., Schmidt, J. A., & Bayne, E. K. (1986) *J. Clin. Invest. 78*, 836–839.

Saklatvala, J., Sarsfield, S. J., & Townsend, Y. (1985) *J. Exp. Med. 162*, 1208–1222.

Schmidt, J. A. (1984) *J. Exp. Med. 160*, 772–787.

Sweet, R. M., Wright, H. T., Janin, J., Chothia, C. H., & Blow, D. M. (1974) *Biochemistry 13*, 4212–4228.

Wang, B. C. (1985) *Methods Enzymol. 115*, 90–117.

Wingfield, P., Graber, P., Movva, N. R., Gronenborn, A. M., & MacDonald, H. R. (1987) *FEBS Lett. 215*, 160–164.